

The Fluctuation Theorem and Dissipation Theorem for Poiseuille Flow

This article has been downloaded from IOPscience. Please scroll down to see the full text article.

2011 J. Phys.: Conf. Ser. 297 012017

(<http://iopscience.iop.org/1742-6596/297/1/012017>)

View [the table of contents for this issue](#), or go to the [journal homepage](#) for more

Download details:

IP Address: 150.203.34.233

The article was downloaded on 17/08/2011 at 05:52

Please note that [terms and conditions apply](#).

The Fluctuation Theorem and Dissipation Theorem for Poiseuille Flow

Sarah J. Brookes

Queensland Micro- and Nanotechnology Centre and School of Biomolecular and Physical Sciences, Griffith University Brisbane, QLD 4111, Australia

E-mail: s.brookes@griffith.edu.au

James C. Reid

Queensland Micro- and Nanotechnology Centre and School of Biomolecular and Physical Sciences, Griffith University Brisbane, QLD 4111, Australia

E-mail: j.reid@griffith.edu.au

Denis J. Evans

Research School of Chemistry, Australian National University, Canberra, ACT 0200, Australia

E-mail: evans@rsc.anu.edu.au

Debra J. Searles

Queensland Micro- and Nanotechnology Centre and School of Biomolecular and Physical Sciences, Griffith University Brisbane, QLD 4111, Australia

E-mail: d.bernhardt@griffith.edu.au

Abstract. The fluctuation theorem and the dissipation theorem provide relationships to describe nonequilibrium systems arbitrarily far from, or close to equilibrium. They both rely on definition of a central property, the dissipation function. In this manuscript we apply these theorems to examine a boundary thermostatted system undergoing Poiseuille flow. The relationships are verified computationally and show that the dissipation theorem is potentially useful for study of boundary thermostatted systems consisting of complex molecules undergoing flow in the nonlinear regime.

1. Introduction

In the last 20 years, considerable advances have been made in the formal study of nonequilibrium systems. Two key advances have been (i) the development of relationships that are valid arbitrarily far from equilibrium so analyses are no longer restricted to the linear response regime, and (ii) the ability to treat finite sized systems, so the thermodynamic limit is not required. In fact, we are now reaching the stage when thermodynamic behavior can be derived from mechanics rather than being based on thermodynamic laws and axioms, and this provides a route to treat the thermodynamics of nonequilibrium systems.

Two important results that have been obtained are the Fluctuation Theorem (FT) [1, 2, 3, 4] and the Dissipation Theorem (DT) [4, 5]. The FT results in an expression for the probability ratio for observing positive and negative values of the dissipation and therefore characterizes fluctuations in the dissipation that occurs in an N-particle system, measured over a finite time. Importantly, it can be used to derive the Second Law of Thermodynamics. The DT provides an expression for the response of arbitrary phase variables to a change in system conditions or application of an external field. Both these results can be obtained using the Liouville equation and the microscopic equations of motion of the particles in the system.

A very general form of the FT was derived in 2000 [6] and has been tested on a wide range of systems. In contrast, a general form of the DT was only published in 2008 [5] and it has not been applied as widely. A special case of the dissipation theorem that is applicable to homogeneously thermostatted systems and has been known for some time [7]. It can be expressed in two forms known as the Kawasaki expression for non-linear response and the transient time-correlation function (TTCF) expression for nonlinear response. The TTCF form has been widely used on homogeneously thermostatted systems, and has not only been shown to be valid, but to provide an efficient computational route to determine the response of a system for low fields. However, the DT has not yet been fully tested on other classes of systems. In this manuscript we will consider application of the FT and the DT to systems undergoing Poiseuille flow: gravity driven flow of a fluid parallel to two thermostatted walls. Atomic fluids and chain polymers are considered at fields ranging from the linear to the nonlinear regime.

2. The Fluctuation Theorem, the Dissipation Function and the Dissipation Theorem

Consider a system that is initially in some known state, which for the purposes of this manuscript can be considered to be an equilibrium state. The system is then subject to a change, such as the application of a gravity field, and the system is monitored for a period, t . If the system is sufficiently small, and the period sufficiently short, the time-averaged properties of the system will take on different values during each time this experiment is repeated. If that is the case, we might be interested in the probability that properties take on particular values during the period t , and also the average response of the system to this field. These probabilities and averages are described by the FT and DT, respectively.

The FT is a well known relationship in nonequilibrium statistical mechanics. It states that time integral of the dissipation function, Ω_t , satisfies the symmetry relation:

$$\frac{Pr(\Omega_t = A)}{Pr(\Omega_t = -A)} = e^A. \quad (1)$$

where $Pr(\Omega_t = A)$ is the probability that Ω_t takes on a value within $A \pm dA$. The FT, (eq. 1) applies to systems starting with a nonequilibrium distribution and relaxing towards equilibrium as time evolves, or those that start in an equilibrium distribution but for $t > 0$, are driven away from equilibrium by boundary conditions (e.g. moving walls) or a mechanical field (e.g. gravity field) as is the case in this paper. The proof of the FT has been given previously (see, for example [2, 4]) and is exceedingly general because it uses so little. In fact, the only feature of the dynamics that is used in the proof is their time reversal symmetry. All microscopic dynamics (quantum and classical) are time reversal symmetric.

The FT has been widely verified both experimentally and computationally for a range of systems. However, difficulty in verifying a relation of the form (1) has been reported in some studies where the subject of the FT, Ω , has been proposed or guessed for a particular system, rather than carefully derived. This is despite the fact that the approach described in [2, 3, 4] leaves no ambiguity as to the function that should satisfy the FT [8]. The time-integral of the

dissipation function, $\Omega_t(\mathbf{\Gamma}(0)) \equiv \int_0^t ds \Omega(\mathbf{\Gamma}(s))$, can be defined as the logarithm of the ratio of the probability of seeing a set of trajectories of duration t , initially centered at a point in N -particle phase space, $(\mathbf{\Gamma}(0))$, to the probability of observing (from the same probability distribution) the conjugate set of anti-trajectories formed from their time-reversal. Here $\mathbf{\Gamma} \equiv (\mathbf{q}, \mathbf{p})$ is a point in phase space where \mathbf{q} is the position and \mathbf{p} is the momentum. Mathematically it is defined as:

$$\Omega_t(\mathbf{\Gamma}(0)) = \ln \left(\frac{f_0(\mathbf{\Gamma}(0))}{f_0(\mathbf{\Gamma}^*(t))} \right) - \Lambda_t(\mathbf{\Gamma}(0)) \quad (2)$$

where the asterisk denotes a time reversal mapping of a point in phase space, $\Lambda = \frac{\partial}{\partial \mathbf{\Gamma}} \cdot \dot{\mathbf{\Gamma}}$ is the rate of phase space compression, $\Lambda_t(\mathbf{\Gamma}(0)) \equiv \int_0^t ds \Lambda(\mathbf{\Gamma}(s))$ and $f_0(\mathbf{\Gamma}(t))$ is the phase space probability density with respect to the distribution at $t = 0$, at a phase $\mathbf{\Gamma}(t)$. Here we will determine the dissipation function for a system undergoing thermostatted Poiseuille flow and find that it is an important physical property of the system.

The DT gives the nonequilibrium average of an arbitrary phase function. Using the FT and the Lagrangian form of the Liouville equation, it only takes a few lines of algebra to derive the DT [4] in its TTCF from as:

$$\langle B(\mathbf{\Gamma}(t)) \rangle_{f_0} = \langle B(\mathbf{\Gamma}(0)) \rangle_{f_0} + \int_0^t ds \langle \Omega(\mathbf{\Gamma}(0)) B(\mathbf{\Gamma}(s)) \rangle_{f_0} \quad (3)$$

where the notion $\langle \dots \rangle_{f_0}$ implies that the ensemble average is with respect to the distribution $f(\mathbf{\Gamma}, 0)$. Equation (3) is exact for arbitrary system size and arbitrarily far from equilibrium.

3. Simulations

3.1. Equations of motion for Poiseuille flow

The FT for Poiseuille flow has been considered previously [9, 10], however, a detailed derivation of the dissipation function was not given. Furthermore, the DT was not tested for this system.

In Poiseuille flow, the system of interest is contained by a slit pore, and a gravity field is applied parallel to the pore walls. In this work, the fluid particles are purely Newtonian, but the temperature of the wall particles is directly controlled by use of a fictitious thermostat. As argued previously [10], this type of construction can be used to provide a realistic model since we can make the thermostat remote from the system of interest, and the system will become insensitive to the details of the thermostat. We set orient the system so that the walls are normal to the z axis and the field acts in the x direction. The equations of motion for the fluid particles can then be written:

$$\begin{aligned} \dot{\mathbf{q}}_i^F &= \mathbf{p}_i^F / m_i, \\ \dot{\mathbf{p}}_i^F &= \mathbf{F}_i^F + F_e \mathbf{i}, \end{aligned} \quad (4)$$

where i is the particle index, the superscript F means that the particle belongs to the fluid, and \mathbf{F}_e is the external force. The forces \mathbf{F}_i^F are due to i interactions of the fluid particle with other particles in the fluid and the wall particles. Details of these interactions will be given in the next sub-section. The equations of motion for the wall particles are given by:

$$\begin{aligned} \dot{\mathbf{q}}_i^W &= \mathbf{p}_i^W / m_i, \\ \dot{\mathbf{p}}_i^W &= \mathbf{F}_i^W - \alpha \mathbf{p}_i^W, \end{aligned} \quad (5)$$

where the superscript W denotes that the particle belongs to the wall. The temperature is controlled by a Gaussian thermostat which fixes the kinetic temperature of the wall through the Lagrangian multiplier $\alpha = \left(\sum_i^{N_W} \mathbf{F}_i^W \cdot \mathbf{p}_i^W \right) / \left(\sum_i^{N_W} \mathbf{p}_i^W \cdot \mathbf{p}_i^W \right)$. In this case, in addition to the interparticle interactions, \mathbf{F}_i^W contains forces applied to tether the wall particles to lattice positions, to create a solid-like wall.

3.2. System parameters

Two types of system are considered in this work - a purely atomic fluid and a fluid consisting of short chain polymers modelled through the Finite Extendable Nonlinear Extendable Elastic Potential (FENE) [11]. All systems were modelled as a slit pore with four wall layers. Each fluid and wall atom in a system interacts via the modified Lennard-Jones potential, the Weeks, Chandler and Andersen potential (WCA) [12, 13]. The WCA truncates the LJ potential at its minimum, so the potential is zero at the cutoff value.

$$\Phi_{WCA}(r_{ij}) = \begin{cases} 4\epsilon \left[\left(\frac{\sigma}{r_{ij}} \right)^{12} - \left(\frac{\sigma}{r_{ij}} \right)^6 \right] + \epsilon, & r_{ij} \leq 2^{\frac{1}{6}}\sigma, \\ 0, & r_{ij} > 2^{\frac{1}{6}}\sigma, \end{cases} \quad (6)$$

where $r_{ij} = |\mathbf{q}_i - \mathbf{q}_j|$ with \mathbf{q}_i being the laboratory particle position, σ is the value of r_{ij} for which the LJ interaction potential is zero, and ϵ is the well-depth of the LJ potential. All the physical units are expressed in reduced units where the unit of mass is the particle mass m , the energy unit is the parameter ϵ and the length unit is σ . To keep the wall atoms at their equilibrium lattice sites, a retarding force in the form of a harmonic potential constraint $U_{harm}(\mathbf{q}_i)$ was used,

$$U_{harm}(\mathbf{q}_i) = \frac{1}{2}k_s(\mathbf{q}_i - \mathbf{q}_{i,eq})^2, \quad (7)$$

where $\mathbf{q}_{i,eq}$ the lattice position of the i^{th} wall atom. A harmonic force constant of $k_s = 15$ was used in the simulations.

The polymers are modelled as a chain of united-atoms where the united atom model represents each carbon group as a single particle and particle are connected using a FENE potential,

$$\Phi_{FENE}(r_{ij}) = \begin{cases} -\frac{1}{2}kR_0^2 \ln \left[1 - \left(\frac{r_{ij}}{R_0} \right)^2 \right], & r_{ij} < R_0, \\ \infty, & r_{ij} \geq R_0. \end{cases} \quad (8)$$

This potential allows the united-atoms to remain bound to one another, and unable to extend beyond $r_{ij} = R_0$. A suitable choice of k and R_0 also ensures the polymer chains cannot cross one another. In this work $k = 30$ and $R_0 = 1.5\sigma$ which has shown to be an appropriate choice in several studies [14, 15, 16].

Each system contains a total of 128 atoms (or united-atoms) with 64 in the walls and the remaining 64 in the fluid. Two polymer systems consist of 4 and 8 united atoms per chain length were simulated and have a total of 16 and 8 molecules respectively. All atoms were initially on an body-centred lattice with an atom density of 0.8, and with periodic boundaries in all dimensions. Within the unit cells, the walls had a surface area of $5.4\sigma \times 5.4\sigma$ and a pore of width 1.7σ . The systems were equilibrated for 20^7 time-steps with the temperature maintained at $T = 1$ using a Gaussian thermostat. After this time, 10^5 transient nonequilibrium trajectories were spawned from the equilibrium trajectory at regular intervals, and the properties measured as a function of time.

4. Results and Discussion

4.1. The dissipation function

In this section we will derive the dissipation function, which is the subject of the FT (eq. 2), for Poiseuille flow. The FT for Poiseuille flow has been considered previously in 1999 [9] and 2001 [10]. The 1999 paper considered an isoenergetic system and the fluctuation relation was determined by considering phase space expansion. This is not possible in thermostatted systems

and the more general approach, via the dissipation function needs to be used. The 2001 paper states the isothermal FT, but does not provide a full derivation. Here we give a complete derivation of the dissipation function to illustrate the application of this approach to a realistic system.

In order to apply the FT, the dynamics must be time reversal symmetric, and this is valid for Poiseuille flow. In addition the dynamics and initial ensemble must be ergodically consistent which implies that all points accessed by the nonequilibrium trajectory are part of the initial ensemble. If the initial ensemble is the isokinetic ensemble, and the dynamics is thermostatted using a Gaussian thermostat, this will be true. The reasons why these requirements are necessary have been discussed in detail in [2, 3, 4].

We consider a system that is initially at equilibrium with walls thermostatted using a Gaussian thermostat (i.e. the system would be modelled with the equations of motion above but with $F_e = 0$). The distribution function for this system is,

$$f(\mathbf{\Gamma}, 0) = \frac{e^{-\beta H(\mathbf{\Gamma})} \delta(K^W(\mathbf{\Gamma}) - K_0)}{Z} \quad (9)$$

where $\beta = 1/k_B T$, k_B is the Boltzmann constant, T equilibrium temperature of the system, $H(\mathbf{\Gamma})$ is the internal energy of the system, $K^W(\mathbf{\Gamma})$ is the kinetic energy of the wall particles, K_0 is the required kinetic energy of the walls, δ is a Dirac delta function and Z is the partition function.

Equation (2) then gives,

$$\Omega_t(\mathbf{\Gamma}(0)) = \ln \left(\frac{e^{-\beta H(\mathbf{\Gamma}(0))} \delta(K^W(\mathbf{\Gamma}(0)) - K_0)}{e^{-\beta H(\mathbf{\Gamma}^*(t))} \delta(K^W(\mathbf{\Gamma}^*(t)) - K_0)} \right) - \Lambda_t(\mathbf{\Gamma}(0)). \quad (10)$$

We note that the internal energy and kinetic energy at a point in phase space and its time-reversed image are the same, that is $H(\mathbf{\Gamma}^*) = H(\mathbf{\Gamma})$ and $K(\mathbf{\Gamma}^*) = K(\mathbf{\Gamma})$. It can also be seen that if the kinetic energy of the walls is fixed at K_0 at equilibrium and during the nonequilibrium trajectory, then both the delta-functions are non-zero and cancel. Furthermore, the phase space expansion rate of the system can be determined from the equations of motion, $\Lambda = \frac{\partial}{\partial \mathbf{\Gamma}} \cdot \dot{\mathbf{\Gamma}} = -(3N_W - 1)\alpha$, so the dissipation function can be expressed:

$$\begin{aligned} \Omega_t(\mathbf{\Gamma}(0)) &= \ln \left(\frac{e^{-\beta H(\mathbf{\Gamma}(0))}}{e^{-\beta H(\mathbf{\Gamma}(t))}} \right) + (3N_W - 1) \int_0^t ds \alpha(\mathbf{\Gamma}(s)) \\ &= \beta H(\mathbf{\Gamma}(t)) - \beta H(\mathbf{\Gamma}(0)) + (3N_W - 1) \int_0^t ds \alpha(\mathbf{\Gamma}(s)) \\ &= \beta \int_0^t ds \dot{H}(\mathbf{\Gamma}(s)) + (3N_W - 1) \int_0^t ds \alpha(\mathbf{\Gamma}(s)) \end{aligned} \quad (11)$$

From the equations of motion, (4) and (5), we can determine the time-derivative of the internal energy $\dot{H} = \sum_{i=1}^{N_F} p_{xi} F_e - 2K_0 \alpha$ and since $2K_0 = (3N_W - 1)k_B T$ we finally obtain,

$$\begin{aligned} \Omega_t(\mathbf{\Gamma}(0)) &= \beta F_e \int_0^t ds \sum_{i=1}^{N_F} p_{xi}(\mathbf{\Gamma}(s)) \\ &\equiv \beta F_e N_F J_{x,t}(\mathbf{\Gamma}(0)) \end{aligned} \quad (12)$$

where we defined the fluid current as $J_x \equiv \sum_{i=1}^{N_F} p_{xi}/N_F$ and therefore $J_{x,t}(\mathbf{\Gamma}(0)) = \int_0^t ds J_x(\mathbf{\Gamma}(s))$. So,

$$\Omega(\mathbf{\Gamma}) = \beta F_e N_F J_x(\mathbf{\Gamma}). \quad (13)$$

This is the dissipation function for Poiseuille flow under boundary thermostatted flow. Importantly in this case the current is the instantaneous current of the fluid particles only,

and the temperature is the kinetic temperature at which the wall particles are fixed using the Gaussian thermostat. Without such a careful derivation these subtle points might not have been anticipated. The temperature that appears can also be identified as the equilibrium thermodynamic temperature to which the system would relax if the field was removed [17].

4.2. Simulation results

In Figure 1 the FT is tested for an atomic fluid with a field of $F_e = 1$, $T = 1.0$ and $n = 0.8$ and a simulation time of $t = 0.4$ for each of 2×10^5 trajectories. The FT would predict that a plot of $\ln(\text{Pr}(\Omega_t = A)/\text{Pr}(\Omega_t = -A))$ versus A would give a straight line with unit slope. Clearly this is consistent with the results. This provides a useful check that the conditions of ergodic consistency and reversibility are being satisfied, that dissipation function has been correctly derived and the simulation code is working properly. As higher fields and/or longer times are considered, it becomes increasingly difficult to observe currentes that oppose the field, and therefore more difficult to validate the FT.

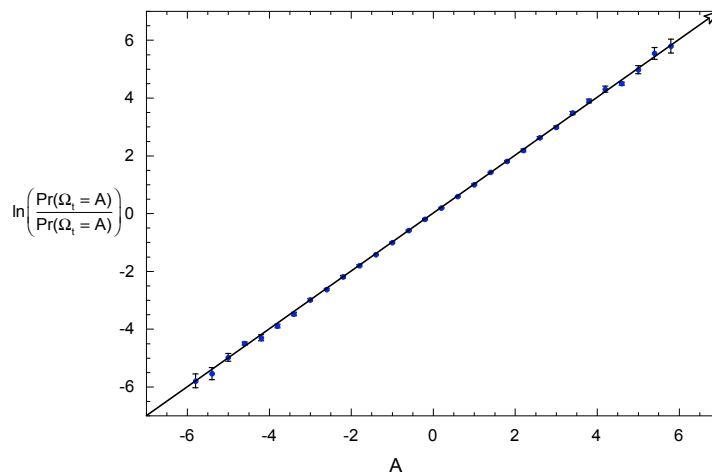


Figure 1. A test of the FT for an atomic fluid with $F_e = 1$, $T = 1.0$ and $n = 0.8$. The results were obtained as the mean of 10 sets of 2×10^4 trajectories of length $t = 0.4$. The error bars are standard error in the mean of these 10 sets of data. The line is the result predicted by the FT.

The fluid current, J_x , through the three systems was examined to demonstrate the validity and utility of the DT. Using the DT (eq. 3) and the dissipation function derived in equation (eq. 13) and also noting that $\langle J_x(\mathbf{\Gamma}(0)) = 0 \rangle$ is zero since J_x is odd with respect to a time-reversal mapping, the TTCF form of the DT for J_x is;

$$\langle J_x(\mathbf{\Gamma}(t)) \rangle_{f_0} = \beta N_F F_e \int_0^t ds \langle J_x(\mathbf{\Gamma}(0)) J_x(\mathbf{\Gamma}(s)) \rangle_{f_0}. \quad (14)$$

Figure 2 shows the response of the current, J_x , determined using (eq. 14) for all three fluids and for a range of applied external fields between 0.01 to 1. There is a monotonic increase in

the current with increase in the applied field at all times. It can be observed that as the length of the polymer increases from a single atom fluid to a 4 atom polymer there is quite a large increase in the current. This is due to the fact that although the atomic number density is held constant, the molecular number density decreases. There is also a smaller increase from the 4 atom polymer to the 8 atom polymer.

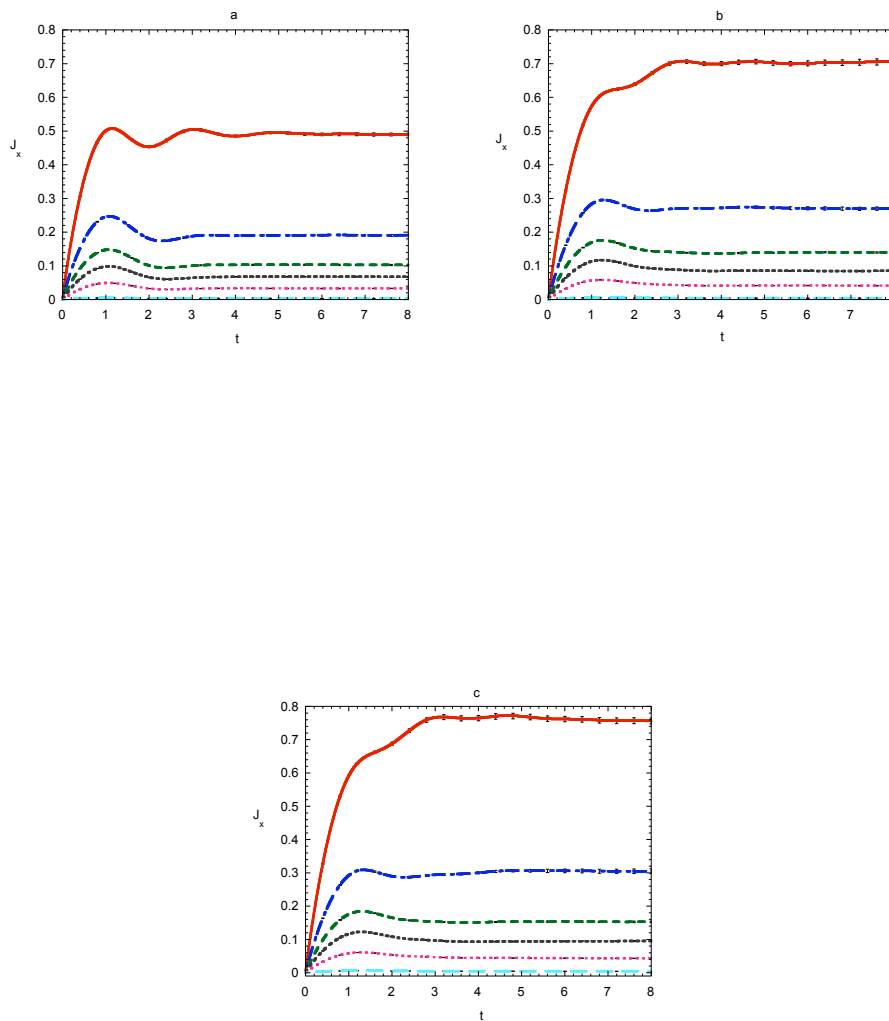


Figure 2. The response of J_x to the application of a range of fields: $F_e = 0.01$ (light blue), $F_e = 0.1$ (pink), $F_e = 0.2$ (black), $F_e = 0.3$ (green), $F_e = 0.5$ (blue), $F_e = 1$ (red). The systems studied were at a temperature of $T = 1$ and an atom density $n = 0.8$ in the fluid and walls for a) an atomistic fluid, b) a 4-atom polymer and c) an 8-atom polymer. Error bars are the standard error in the mean from 10 sets of data.

One of the advantages of using (eq. 3) to calculate properties is its ability to treat small fields. In most cases, nonequilibrium molecular dynamics (NEMD) simulations use a direct averaging method to calculate properties of a nonequilibrium state: that is one simply averages the property over the number of trajectories to get $\langle J_x(t) \rangle$. At large fields the signal to noise ratio is large. Consequently, for strong fields evaluation of properties using the TTCF form of the DT (3) is expected to give the same results for the current as obtained from the direct averaging of NEMD simulations. This can be observed in Fig. 3 where the J_x has been plotted over time for $F_e = 1$ for the 4 atom polymer system. The trajectories are very similar both in the transient time period where the field is first turned on and the steady state where the system has relaxed.

In contrast, at small fields the signal to noise ratio can become so small that the signal is hard to distinguish if direct averaging is used. Therefore for weak fields the DT expression allows the average response to be accurately determined, as is illustrated in Fig. 3b) where J_x has been plotted for a 4 atom polymer with an applied external field of $F_e = 0.01$. The directly calculated J_x for the same system and field is also shown. The shape of the graph obtained using the DT is clearly the same as those for the larger fields (Fig. 3a), again with very little error observed. In contrast the direct calculation give data with a much larger statistical error for the same number of trajectories. The DT can therefore give us reliable data to examine the effects of confinement on the response of a system when a weak external field is applied.

In Figure 4a, J_x/F_e was determined for all applied external fields ranging from 0.01 to 1 for the atomic and polymer systems. There is a reduction in J_x/F_e as the polymer length decreases. This would indicate that the larger polymer is able to move more freely and is again consistent with the reduced molecular number density. It can also be observed that the size of the linear response regime decreases as the polymer length increases. Already for the polymer with 8 united-atoms, the statistical error from direct calculations will be too large to determine the response accurately for low fields using the large number of trajectories averaged in this work. This is not a problem if the system is in the linear regime as the current can simply be extrapolated using the linearity of the response. However, extrapolation is not possible in the nonlinear regime. As much larger polymers are considered, the fields where the system is still in the non-linear regime will become increasingly wide [18]. Then, use of the TTCF form of the dissipation function will be essential. The J_x/F_e response of the 8 atom polymer is best observed in figure 4b where the J_x/F_e is plotted as a function of time. A distinct difference in each field can be seen.

Other properties of the system can be determined in the same manner, using the general equation (3). Here we consider the average Irving-Kirkwood expression for the fluid pressure, p [19]. Figure 5 shows the average pressure of the fluid in the 4 atom polymer with $F_e = 1$ and $F_e = 0.3$. As with the current, when the higher field is applied the direct calculation and the DT expression give similar results. However the DT approach shows a noticeably smoother curve with less error at the lower field.

5. Conclusions

The dissipation function for a system undergoing wall-thermostatted Poiseuille Flow has been derived and was shown to satisfy the FT. The form of the dissipation function for this combination of dynamics and ensemble is unique and is found to be $\beta F_e N_F J_x$ where β is the kinetic temperature of the walls and corresponds to the temperature that the system would relax to if the field was removed [17]. Clearly this is equal to the average entropy production rate at low fields. At higher fields it becomes impossible to define either the entropy or the temperature. In fact there are large “temperature” gradients in the system at higher field strengths and one does not even know where the “temperature” should be measured! The DT rigorously avoids these pitfalls and gives an exact answer even at arbitrarily high values of the driving field. Had

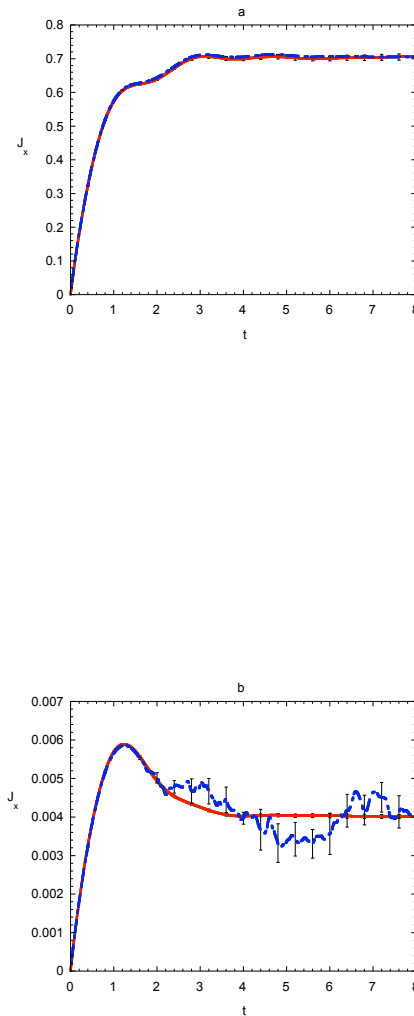


Figure 3. The response of J_x to the application of a field determined using direct calculations (blue) and the TTCF form of the DT (red). The systems studied were at a temperature of $T = 1$ and an atom density $n = 0.8$ in the fluid and walls. In a) a field of $F_e = 1$ is used. In this case the agreement between the two approaches is so high that the two lines are superimposed over most of the trajectory. Error bars are shown and are the standard error over 10 sets of data, but are mostly smaller than the line-width. In b) a field of $F_e = 0.01$ is used. Error bars are shown and are the standard error over 10 sets of data. The error bars are mostly smaller than the line-width for the DT results.

we employed a Nosé-Hoover thermostat the kinetic temperature of the thermostatted particles would have been replaced by the target temperature in the Nosé-Hoover feedback mechanism.

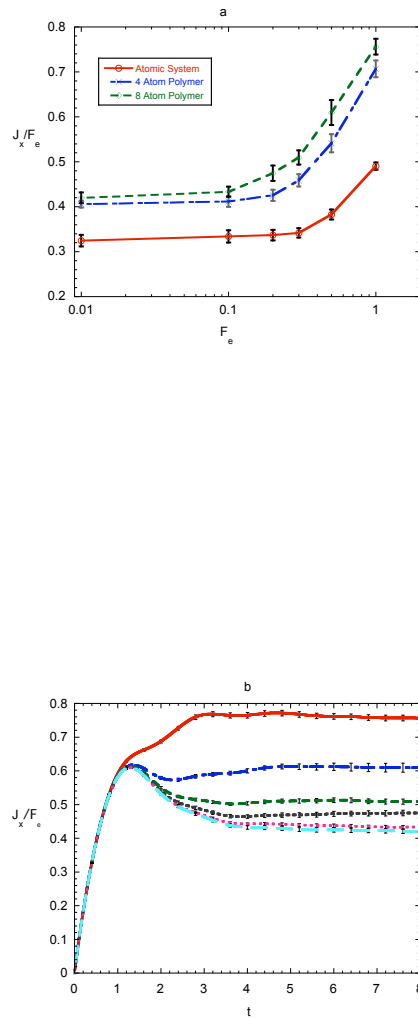


Figure 4. a) The value of J_x/F_e as a function of the field for a range of fields between $F_e = 0.01$ and $F_e = 1$ for the atomic fluid, 4-atom polymer fluid and 8-atom polymer fluid. The systems studied were at a temperature of $T = 1$ and an atom density $n = 0.8$ in the fluid and walls. Error bars are shown for all fields and are the standard error over 10 sets of data. The lines provide guides to the eye. b) The full response curve for the 8-atom polymer under the same conditions. Field range from $F_e = 0.01$ (light blue), $F_e = 0.1$ (pink), $F_e = 0.2$ (black), $F_e = 0.3$ (green), $F_e = 0.5$ (blue) to $F_e = 1$ (red).

The kinetic temperature of the thermostatted particles would not necessarily be the same as the corresponding temperature for the isokinetic system. The actual temperature appearing

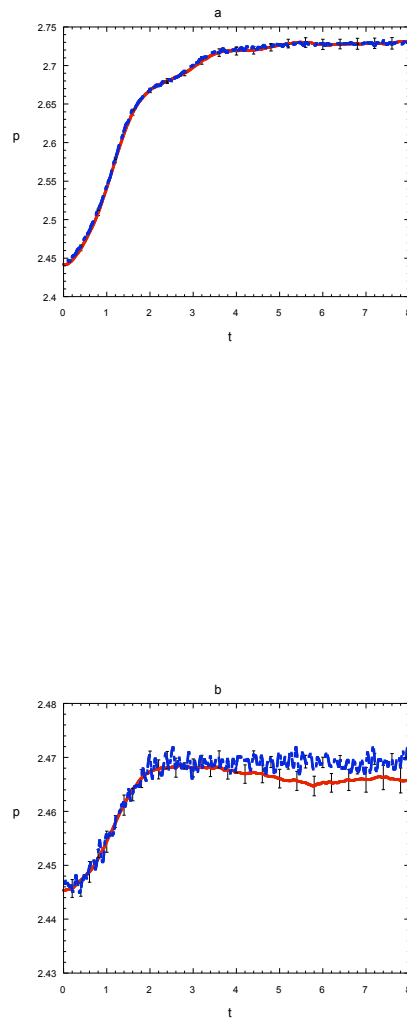


Figure 5. The response of the average Irving-Kirkwood pressure to the application fields: a) $F_e = 1$ and b) $F_e = 0.3$ determined using a direct calculation (blue) and the TTCF form of the DT (red). The systems studied were at a temperature of $T = 1$ and an atom density $n = 0.8$ in the fluid and walls. Error bars are shown and are the standard error over 10 sets of data.

in the DT is in fact always equal to the equilibrium thermodynamic temperature the system would relax to if the driving field was set to zero and the entire system was allowed to relax to equilibrium as is proved in the Relaxation Theorem [20]. The dissipation function has also been applied to calculate the current in both atom and polymeric systems using the DT, validating

this approach for wall-thermostatted systems for the first time. The results showed that as the size of the molecule increase from a single atom to a 4-atom polymer there is an increase in the current with a smaller increase from the 4-atom to the 8-atom polymer. Furthermore the dependency on molecular size was also noted when the atomic system entered the linear regime at larger applied field. As well as providing accurate results over the range of fields considered, the DT approach for calculating averaged properties of systems was clearly advantageous for small fields. For complex molecules where the nonlinear regime occurs are relatively low fields, it will become essential to use the TTCF form of the DT instead of the direct calculations in order to determine properties accurately.

Acknowledgments

The authors would like to thank Griffith University for computational time on their V20z Cluster and support through ARC LIEF and Discovery Grants.

References

- [1] Evans D J and Searles D J 1994 *Phys. Rev. E* **50** 1645
- [2] Evans D J and Searles D J 2002 *Adv. Phys.* **51** 1529
- [3] Sevick E M, Prabhakar R, Williams S R and Searles D J 2008 *An. Rev. Phys. Chem.* **59** 603
- [4] Evans D J, Willams S R and Searles D J 2010 *Thermodynamics of Small Systems, in Nonlinear Dynamics of Nanosystems* Editors Radons G, Schuster H G and Rumpf B (Weinheim: Wiley-VCH), 75-109
- [5] Evans D J, Searles D J and Willams S R 2008 *J. Chem. Phys.* **128** 014504
- [6] Searles D J and Evans D J 2000 *J. Chem. Phys.* **113** 3503.
- [7] Evans D J and Morriss G P 2008, *Statistical Mechanics of Nonequilibrium Liquids 2nd Ed.* (Cambridge: Cambridge University Press)
- [8] We note that in some cases, although the dissipation function can be formally written, it is difficult to test experimentally. In these cases proposal of a similar, experimentally measurable quantity is justified.
- [9] Ayton G S and Evans D J 1999 *J. Stat. Phys.* **97** 811
- [10] Ayton G, Evans D J and Searles D J 2001 *J. Chem. Phys.* **115**, 2033
- [11] Kröger M 2004 *Phys. Rep.* **390** 453
- [12] Weeks J D, Chandler D and Andersen H C 1971 *J. Chem. Phys.* **54** 5237
- [13] Heyes D M and Okumura H 2006 *Mol. Sim.* **32** 45
- [14] Grest G S and Kremer K 1986 *Phys. Rev. A* **33** 3628
- [15] Kremer K and Grest G S 1990 *J. Chem. Phys.* **92** 5057
- [16] Bosko J T, Todd B D and Sadus R J 2004 *J. Chem. Phys.* **121** 1091
- [17] Evans D J, Williams S R and Searles D J 2011 "A proof of Clausius's Theorem for time reversible deterministic microscopic dynamics" *J. Chem. Phys.* submitted
- [18] Cui S T, McCabe C, Cummings P T and Cochran H D *J. Chem. Phys.* **118** 8941
- [19] The Irving-Kirkwood expression for the pressure is simply used as a sample phase variable. It should be noted that if an accurate measurement of the pressure is required, the method of planes should be used. See Todd B D and Evans D J 1997 *Mol. Sim.* **17** 317
- [20] Evans D J, Searles D J and Williams S R 2009 *J. Stat. Mech.* **2009** P07029